

Evaluation of Reinforcement Corrosion in Cementitious Composites Modified with Water Treatment Sludge

Mariana A. M. Rezende,^{1b} Pedro P. Gromboni,^a Patricia G. Corradini,^{1b}*,^{b,c}
Almir Sales^{1b} and Lucia H. Mascaro^{1b}

^aDepartamento de Engenharia Civil, Universidade Federal de São Carlos,
Via Washington Luís, km 235, 13565-905 São Carlos-SP, Brazil

^bDepartamento de Química, Universidade Federal de São Carlos,
CP 676, 13565-905 São Carlos-SP, Brazil

^cLaboratório de Análises Químicas e Agroambientais (LAQUA), Instituto Federal de Educação,
Ciência e Tecnologia Fluminense, Campus Itaperuna, BR 356, km 3, 28300-000 Itaperuna-RJ, Brazil

The water treatment sludge (WTS) is a residue composed of organic and inorganic matter in a solid, liquid, and gaseous state that has a variable composition concerning its physical, chemical, and biological characteristics. The irregular disposal of WTS can promote harmful changes to the environment, such as reduction of dissolved oxygen and increase in the concentration of aluminum and other metals in the receiving watercourses. To propose a suitable purpose for this residue, this work evaluated the physical and mechanical properties of the concrete and corrosion resistance of the reinforcement in a cementitious composite using WTS in replacement to the natural sand. A conventional concrete and a conventional mortar were used as a reference and a 3% WTS-content concrete, and a 3% WTS-content mortar were prepared to evaluate the WTS influence in mechanical properties and corrosion resistance. By electrochemical measurements, it was observed that the resistance of the cementitious matrix was not altered by WTS addition. Regarding steel resistance, the WTS may promote a higher susceptibility to frame corrosion, which can be correlated to the lower pH than reference medium (REF). The concrete reinforcement characterization indicates that concretes with WTS can be used as reinforced concrete structure in urban areas.

Keywords: reinforcement corrosion, water treatment sludge, sustainable aggregate, modified cementitious matrix

Introduction

The irregular disposal of water treatment sludge (WTS) can promote harmful changes to the environment. Brazil has around 7,500 water treatment plants (WTP) and all treatment plants produce wastes in the process of purifying water for human consumption.¹ In developing countries, water treatment wastes are generally disposed of in the same rivers and streams that supply water for the treatment because there is no suitable technology to designate this waste.² The majority of WTP waste is a sludge retained in decanters and a strategy to correctly dispose of this sludge is a challenge for WTP managers.³

WTS is a residue composed of organic and inorganic matter in a solid, liquid, and gaseous state that has a variable composition concerning its physical, chemical, and biological characteristics. Among the harmful changes to the environment caused by the irregular disposal of WTS are the reduction of dissolved oxygen and the increase in the concentration of aluminum and other metals in the receiving watercourses creating a major impact on the environment.⁴

Among the possible recycling alternatives currently existing for WTS are the recovery of aluminum present in the sludge and its use in the treatment of domestic effluents,⁵ the spreading of sludge in the soil for agricultural purposes and the recovery of degraded areas,⁶ and the application of sludge as a supplementary cementitious material.^{7,8}

The application of WTS in civil construction can be beneficial for another reason: to reduce the extraction of

*e-mail: patricia.corradini@ifff.edu.br

Editor handled this article: Rodrigo A. A. Muñoz (Associate)

raw materials, such as sand and gravel.⁹⁻¹¹ Figure 1 presents the numbers of sand and gravel extraction, according to the United States Geological Survey. An increase since 2008 has been observed, reaching approximately 330 million tons in the years 2018 and 2019. This number has not been maintained in 2020 due to the decrease in industrial production arising from the COVID-19 pandemic.^{12,13} Although Figure 1 illustrates the total extraction of sand, which serves several industrial processes, the area of civil construction also has a large share of contribution. According to the United States Geological Survey, the total sand and gravels used only for construction was 265 million metric tons in 2020.¹²

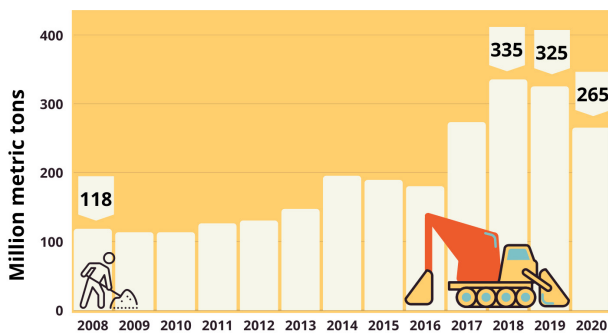


Figure 1. Industrial sand and gravel production worldwide, according to the United States Geological Survey (adapted from reference 12).

The extraction process cause decrease in the availability of these materials on the market and an increase in their price, for example, in the United States of America (USA), the price of sand and gravel increased about 30% from 2010 to 2020.¹² Besides, natural sand sometimes has to be transported from the extraction region to the region of use which means that its price can be even higher, the further from the extraction it is taken. Recycled sands, on the other hand, can be used conveniently in the origin region of the waste. Therefore, attempts to replace natural aggregates with recyclable ones are necessary. Brazil, like most countries where there is water treatment, has WTP in all its political regions, therefore, WTS is a waste present throughout the Brazilian territory, unlike natural sand.

Kaish *et al.*¹⁴ investigate the properties of concrete after the alum sludge incorporation as partial replacement of fine aggregate. The authors showed that the optimum replacement must not exceed 10% of sludge, to ensure the strength and concrete durability proprieties. Ching *et al.*¹⁵ studied the effect of mix proportions of alum sludge in concrete and evaluated different mechanical and physical properties, such as slump behavior, compressive and flexural strength, water absorption and chloride penetration. They concluded that 4% of addition is the higher concentration to applied in the concrete.

Despite some studies trying to add recyclable materials to the concrete, there was no replacement of sand, only is applied to mortar modifier. Considering the need to properly dispose the WTS and the need to apply recycled sands in civil construction, in this research, the physical and mechanical properties of the concrete, as well as the corrosion resistance of the reinforcement in a cementitious composite using WTS in replacement to the natural sand were studied, aiming to evaluate the effect of adding this material in concrete.

Experimental

Materials

The materials used in this study were: (i) Portland cement with a high early strength sold by Holcim do Brasil in São Carlos, Brazil (chemical composition of (wt.%) 64.0% CaO, 19.2% SiO₂, 5.0% Al₂O₃, 3.2% Fe₂O₃, 2.8% SO₃, 2.4% CO₂, 0.6% MgO, 0.6% K₂O, and 0.1% Na₂O); (ii) quartz sand and basalt stone obtained from the São Carlos city area (Brazil); (iii) water treatment sludge (WTS) and (iv) commercial carbon steel for civil construction used in Brazil (named CA-60) sold by Gerdau Brasil in São Carlos, Brazil.

The commercial carbon steel used is a corrugated steel rebar (AISI 1005, 5 mm-diameter). The chemical composition of the AISI 1005 was determined by atomic absorption spectroscopy (Inductar CS cube analyser') as follows (wt.%): 99.098% Fe, 0.054% C, 0.384% Mn, 0.027% P, 0.036% S, 0.081% Si, 0.077% Cr, 0.059% Ni, 0.014% Mo and 0.170% Cu.

The sludge used in this research was collected from the São Carlos Water Treatment Plant in the state of São Paulo, Brazil. This WTP treats 500 L s⁻¹ of water in a traditional system that has the following steps: coagulation (using Al₂(SO₄)₃ as a coagulant), flocculation, sedimentation, and filtration. It is in the decanter that the sludge is deposited in the tank bottom by gravity. In a year, the São Carlos WTP produces 1500 m³ of sludge, which is removed every three months. A schematic of the São Carlos water treatment plant, with more details of the water station is available in Figure S1 in the Supplementary Information (SI) section.

In the laboratory, the sludge collected at WTP was placed on metal trays for 48 h for water evaporation at room temperature. After that, WTS was completely oven-dried at 110 °C for 24 h in the oven with air circulation and air renewal Marconi MA 035 (Piracicaba, Brazil). The WTS was standardized by sieving (with a 4.8 mm mesh) and grinding in an aggregate crusher Marconi MA-590/SE

(Piracicaba, Brazil). Figure S2 (SI section) shows WTS ready to use and quartz sand for visual comparison.

According to Cordeiro,¹⁶ São Carlos WTP performs a three-months washing of the decanters in a traditional way (in large intervals of time), causing an accumulation of sludge at the bottom of the tank that occupies a considerable volume, therefore leading to an increase in the concentration of solids. Besides, the concentrations of metals are higher in systems like these, therefore the irregular disposal causes a greater environmental impact. Table 1 presents the physicochemical characteristics of a sample from the WTS collected in São Carlos WTP.¹⁶

Table 1. Physicochemical characteristics of water treatment sludge from São Carlos (SP, Brazil) made available by Cordeiro¹⁶

Sample characterization ^a	Value
pH	7.20
Chemical oxygen demand / (mg L ⁻¹)	4800
Total solids / (mg L ⁻¹)	58.630
Suspended solids / (mg L ⁻¹)	26.520
Dissolved solids / (mg L ⁻¹)	32.110
Aluminum / (mg L ⁻¹)	2.16
Zinc / (mg L ⁻¹)	4.25
Lead / (mg L ⁻¹)	1.60
Cadmium / (mg L ⁻¹)	0.02

^aTurbidity and color are not determined on concentrated sludge.

Concrete mixtures

WTS was used as fine aggregate in partial substitution to natural sand (levels of 3% by weight). This content was chosen from the results achieved by previous studies in our group considering maximum reuse of sludge.²

Four groups of cementitious composites were prepared. A conventional concrete (REF-c) and a conventional mortar (REF-m) were used as a reference and a 3% WTS-content concrete (WTS-c) and a 3% WTS-content mortar (WTS-m) were prepared to evaluate the WTS influence on mechanical properties and corrosion resistance. Table 2 shows the

proportion of materials used in each group of cementitious composites, the consistency of the concretes, recommended by NBR NM 67.¹⁷

Methods

Concrete and mortar mixtures were made using a mechanical mixer Lider (São Paulo, Brazil) to obtain a homogeneous mass. For physical and mechanical properties tests, cylindrical specimens of concrete measuring 100 mm (diameter) × 200 mm (height) were molded (Figure S3, SI section). Samples were kept in the wet chamber until the time of testing to cure according to the Brazilian standard NBR 9479.¹⁸ Concrete samples were submitted to the following tests: water absorption, voids, and specific gravity according to NBR 5739;¹⁹ compressive strength, modulus of elasticity, and tensile strength according to NBR 8522,²⁰ NBR 7222²¹ and NBR 9778,²² respectively.

For electrochemical analysis, specimens of prismatic mortars measuring 100 mm (height) × 70 mm (width) × 50 mm (depth) were molded with two rebars inside. After mortar demolding, copper cables were connected to the sample reinforcements to ensure electrical contact (Figure S3). The corrugated steel was cut into 10 cm bars, as the working electrode (WE), and the sample was cleaned following ASTM G1-03²³ and an area of 6.28 cm² was exposed insulating the rest of the bars with epoxy resin.

The electrochemical characterizations were performed in a conventional three-electrode glass cell, at 23 °C, using an Autolab-PGSTAT20 potentiostat/galvanostat equipped with a FRA32 module. A titanium cylinder was used as the auxiliary electrode (AE). Hg/HgO|KOH (1 mol L⁻¹) was employed as the reference electrode (RE) for passivation analysis and a saturated calomel electrode (SCE) was employed as the RE for the corrosion analysis.

Electrochemical impedance spectroscopy (EIS) was performed on mortar steels at the open-circuit potential (OCP) in the 100 kHz to 10 mHz frequency range, applying a 10 mV of AC modulation. Frequency sampling was

Table 2. Mix proportion of materials to produce the cementitious composites

Group	WTS content / %	Mix proportion (by mass)					Consistency / mm
		Cement	WTS	Sand	Basalt	w/c	
REF-c	–	1.00	0.00	2.00	3.00	0.53	50
REF-m	–	1.00	0.00	2.00	–	0.53	279
WTS-c	3	1.00	0.06	1.94	3.00	0.54	50
WTS-m	3	1.00	0.06	1.94	–	0.54	290

WTS: water treatment sludge; REF-c: conventional concrete; REF-m: conventional mortar; WTS-c: 3% WTS-content concrete; WTS-m: 3% WTS-content mortar; w/c: water to cement ratio.

6 points *per decade*. All the EIS spectra were curve-fitted using Nova 2.1.4 software. The OCP of the rebar was monitored for 24 consecutive days while the mortar samples were completely submerged in $\text{Ca}(\text{OH})_2$ saturated solution. For corrosion potential measurement the ASTM C876-15 was followed.²⁴

The *ex-situ* characteristics of the WE surface in the different mortar samples were conducted at different periods of immersion in $\text{Ca}(\text{OH})_2$ saturated solution (commercial purity, Synth, Diadema, Brazil). For that, morphology and elemental composition of the passive films formed were investigated using scanning electron microscopy (SEM) with high-resolution field emission using and FEG-SEM ZEISS SUPRA 35, coupled to energy dispersive spectrometry. The morphology of the WE in mortar samples immersed in a 3.5% NaCl solution (commercial purity, Synth, Diadema, Brazil) were investigated using SEM at the end of the corrosion potential experiment.

Results and Discussion

Physical and mechanical properties

The results for the physical properties of concrete samples are shown in Table 3. The average value of three samples for water absorption for water treatment sludge concrete (WTS-c) is 1.2% lower than the average value of three samples for reference concrete (REF-c), showing that the pore volume of these concretes is similar. Ching *et al.*¹⁵ observed the same behavior, replacing Portland cement by 2-8% of WTS, and the higher the WTS content, the lower the water absorption and the porosity. Analogously, the ratio of permeable pore volume and total volume of the concrete sample (voids) for the WTS-c is 2.6% lower

than for the REF-c and the specific gravity is 1.3% lower for WTS-c than for REF-c, possibly because WTS acted as a filler. Therefore, WTS-c group did not present a significant difference in physical property results compared to the reference concrete and the value obtained was the expected for the water to cement ratio (w/c) according to the literature.^{14,15,25-27}

Table 4 shows the mechanical properties of the concrete samples after 28 curing days in the moist room. Compressive strength of WTS-c corresponds to almost 88% of the compressive strength of REF-c, which may be related to the increase in w/c ratio in WTS-c samples in the mixtures to reach the same consistency as the REF-c samples. Kaish *et al.*¹⁴ observed that by incorporating 5 and 10% of WTS in replacement of fine aggregate, the compressive strength of the concrete in 28 days was similar to the control sample. However, the w/c was the same. Modulus of elasticity showed a decrease from REF-c to WTS-c of around 5% and tensile strength of around 14%, both believed to be caused by the higher w/c either. These average values of mechanical properties in WTS-c show that possibly this concrete with 3% of sludge cannot be used in the marine environment according to Brazilian standard NBR 6118,²⁸ which explains that if the concrete will be in a marine environment, it must have a compressive strength of at least 30 MPa, only reached by the REF-c.

Although no research was found replacing WTS by aggregates or incorporating it in concrete as aggregate, some research used WTS in bricks, clay, and paving blocks²⁹⁻³² and demonstrated that the increase of WTS content decreased the strength and increased water absorption in elements. Some research was made using WTS fired up to 850 °C as supplementary cementitious material^{33,34} and concluded that the use of 5 and 10% by

Table 3. Physical properties average value of concrete samples

Group	Water absorption			Average value / %	Voids		Average value / %	Specific gravity	
	Average value / %	SD / %	CV / %		SD / %	CV / %		SD / %	CV / %
REF-c	5.15	0.40	7.76	12.31	0.90	7.29	2.39	0.01	0.51
WTS-c	5.09	0.16	3.05	11.99	0.34	2.81	2.36	0.01	0.25

SD: standard deviation; CV: coefficient of variation; REF-c: conventional concrete; WTS-c: 3% WTS-content concrete.

Table 4. Mechanical properties of the concrete samples after 28 curing days

Group	Compressive strength			Modulus of elasticity			Tensile strength		
	Average value / MPa	SD / %	CV / %	Average value / MPa	SD / %	CV / %	Average value / MPa	SD / %	CV / %
REF-c	30.2	1.1	4	30.2	1.1	4	30.2	1.1	4
WTS-c	26.5	0.7	3	26.5	0.7	3	26.5	0.7	3

SD: standard deviation; CV: coefficient of variation; REF-c: conventional concrete; WTS-c: 3% WTS-content concrete.

cement weight of WTS increased the compressive strength. In this work, the strength decreased with the incorporation of WTS, but water absorption did not.

Mortar monitoring in alkaline medium

EIS measurements are useful to obtain information on electrochemical systems, such as the presence of surface passivation films, interfacial corrosion, and mass transfer phenomena. In this way, this technique was used to follow the curing process, i.e., in the first 24 days after the mortar casting. All EIS measures were performed in $\text{Ca}(\text{OH})_2$ saturated solution. The Nyquist diagrams for REF-m and WTS-m are presented in Figure 2. Both mortars showed the same behavior: a semicircle, indicating the occurrence of resistive and capacitive effects. At high frequencies (ca. 400 Hz) it is possible to observe the formation of a small semi-circle, in both mortar systems (see Figure S5,

in SI section). Over time, it is possible to observe that the radius of the semi-circle increases, indicating the formation of the passive film on the steel. The equivalent circuit model, used to fit the EIS spectra, is shown in Figure 2c. Some works in the literature explain the all-electrical phenomena involved,³⁵⁻³⁸ but in this study, we will focus on R_2 and R_3 , which in practical terms can be related to the cement matrix resistance and steel corrosion resistance, respectively. As seen in Figure 3, the addition of WTS does not alter the resistance of the cementitious matrix, indicating that the microstructure compaction is similar for both REF and WTS. Regarding steel resistance, the difference of corrosion resistance indicates that the WTS may promote a higher susceptibility to frame corrosion. It is interesting to notice that R_3 increases faster in REF-m compared to WTS-m, and at 7 days of immersion in $\text{Ca}(\text{OH})_2$ saturated solution, the steel in WTS-m reached a plateau of the passivation film growth. Therefore, suggesting that WTS-m

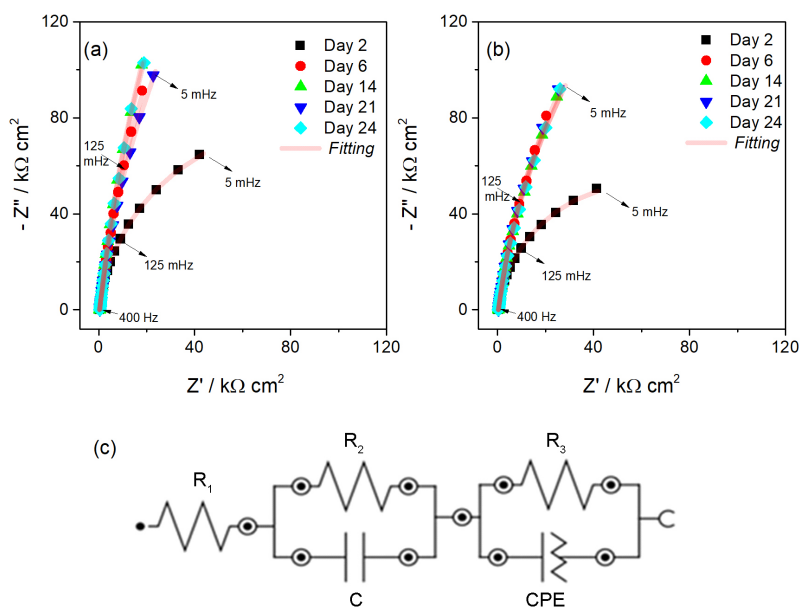


Figure 2. Nyquist diagrams for (a) REF-m and (b) WTS-m, all in $\text{Ca}(\text{OH})_2$ solution. (c) Representation of the equivalent circuit used to fit the EIS data of rebars.

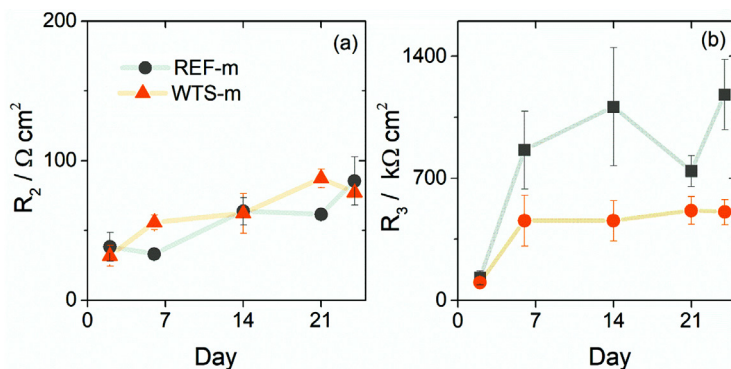


Figure 3. Cement matrix resistance (R_2) and steel corrosion resistance (R_3) values obtained fitting the equivalent circuit (Figure 2c) as a function of the immersion time in $\text{Ca}(\text{OH})_2$ solution.

provides an environment that makes the steel less capable to passivate.

Figure 4 shows the average of three open-circuit potential measured values for REF and WTS-m samples using Hg/HgO as reference electrode. OCP started in -42 and -66 mV for REF-m and WTS-m, respectively. Then, the two mortars showed shift to more negative OCP values. OCP of REF-m stabilized at approximately -130 mV between the 8th and 18th day and increased to stabilize on the 20th day with OCP at approximately -120 mV until the end of the experiment (24th day). OCP of WTS-m stabilized at around -225 mV from day 1 to 6 and increased to -150 mV on the 21st day. WTS-m's potential stabilized in -175 mV on 21st day until the end of the experiment. So, both samples presented their OCP stabilized, suggesting that the passivation film was formed, but REF-m samples stabilized before than WTS-m. Furthermore, WTS-m stabilized in a more negative potential than REF-m, suggesting that WTS-m is more susceptible to corrosion than REF-m. The decrease in the OCP at the beginning of the experiment done in this work in an alkaline solution was observed by some researchers³⁹⁻⁴² and may be associated with the oxygen depletion at the steel-mortar interface because of the difficulty in mass transportation.

After opening the mortars to remove the steel bars from the samples scanning electron microscopy (SEM) images were taken on an as-received steel sample (blank sample), on steels from REF-m samples (REF) at 7 and 21 days of immersion in $\text{Ca}(\text{OH})_2$ saturated solution and on steel from WTS-m sample (WTS) at 7 and 21 days of immersion in $\text{Ca}(\text{OH})_2$ saturated solution, as can be seen in Figure 5. Figure 5a shows the blank sample, as can be seen only steel scratches from the cleaning process. After 7 days of immersion in alkaline solution, the steel surface in Figure 5b shows that the REF sample presents a coating structure

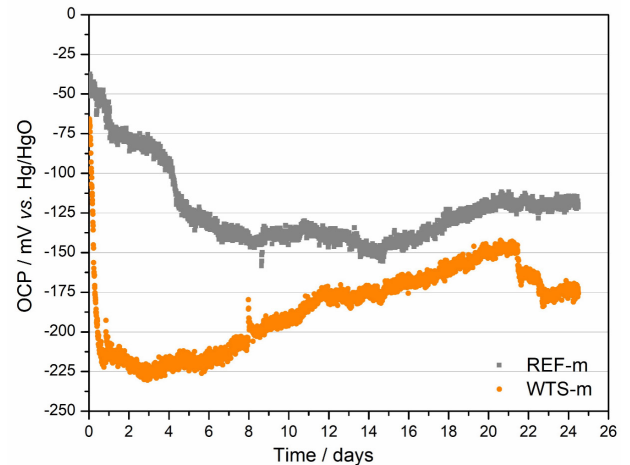


Figure 4. Average of three open-circuit potentials measure values as a function of immersion time of REF and WTS-m samples in $\text{Ca}(\text{OH})_2$ saturated solution.

formed clearly. A similar structure was observed in the REF sample after 21 days of immersion in $\text{Ca}(\text{OH})_2$ saturated solution. These structures are probably the passivating film given that EIS and OCP measurements indicated a passivation process at this age. For the WTS sample on the 7th day, it is possible to see that a structure is forming, but it still does not cover the sample well, as happened for REF, at this age. On the 21st-day WTS sample presented a well-developed coating that better covers the surface than before. Nevertheless, this coating does not cover all the steel surface and evidencing what was observed in the monitoring of the OCP (Figure 3) that the passivating film was not well-formed after 21 days of immersion in the alkaline solution.

Energy dispersive X-ray (EDX) measurements also were performed and are presented in Figure S6 (in SI section). The presence of calcium, carbon, oxygen and iron indicates that most of the formed precipitate is calcium carbonate and iron oxy-hydroxide. This is in agreement with the work

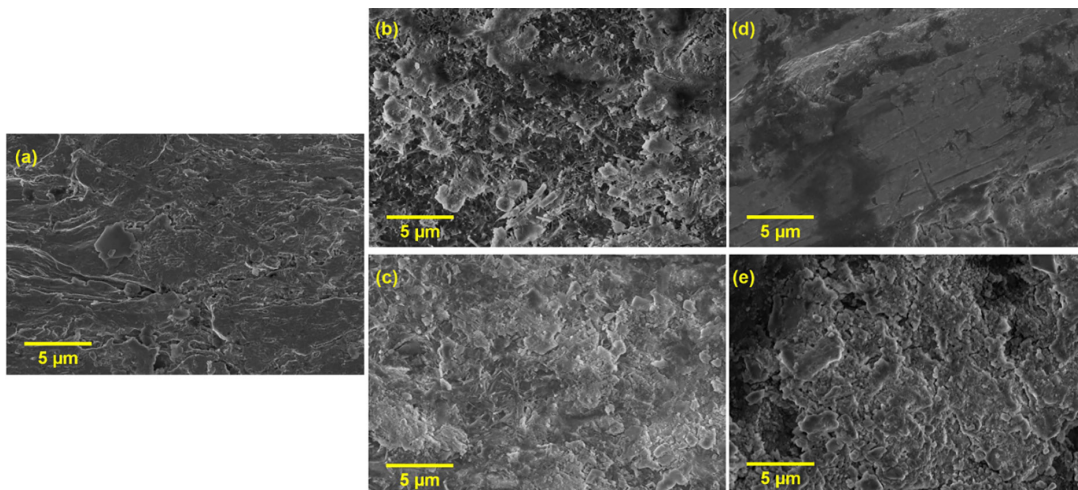


Figure 5. SEM images of (a) blank sample, (b) REF 7th day, (c) REF 21st day, (d) WTS 7th day and (e) 21st day.

of Gromboni *et al.*,⁴³ who observed that most of the films obtained under similar study conditions are amorphous or nanocrystalline. Figure S6 also indicates that with an increase in mortar curing, there is a change in the protective film, decreasing the proportion of CaCO_3 , and increasing the contribution of iron oxides and oxy-hydroxide.

Mortar monitoring in chloride medium (corrosion initiation)

To evaluate the corrosion potential of reinforcing steel in WTS and WTS-free mortars, the specimens were immersed at half height in 3.5% NaCl solution for two days and oven-dried at 50 °C for five days every week for 39 weeks. As the mortars were being immersed in NaCl solution, NaCl salts were crystallizing in mortar pores, increasing compactness in all specimens. Figure 6 shows that as the cycles go by, the masses of samples increased. This effect was caused by the accumulation of NaCl into the mortar microstructure and consequently the water retention. After around 32 cycles the mass variation started to stabilize suggesting that the pores were clogged with salt and the penetration of more NaCl solution became difficult.

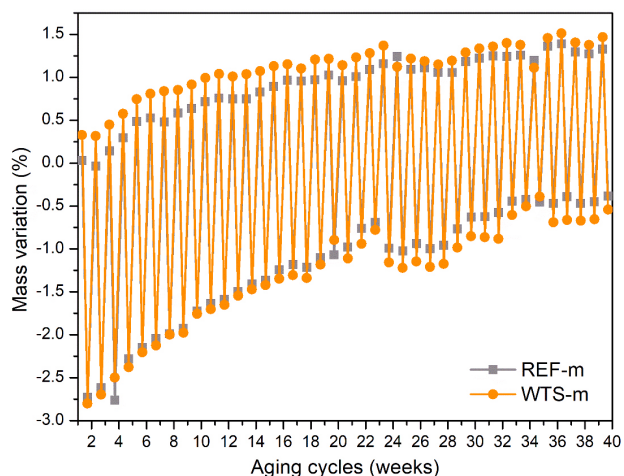


Figure 6. Variation in the mass of REF-m and WTS-m specimens during aging cycles. Higher (lower) values refer to saturated (dried) conditions.

Corrosion potentials of reinforcing steel in WTS and WTS-free mortars were measured and compared to the empirical limits established by ASTM C876-15²⁴ as shown in Figure 7. However, it is used as an eye guide because its applicability to alternative cementitious composites such as WTS-m is not defined. If the OCP > -104 mV vs. Ag/AgCl/KCl sat., there is 90% probability of having no corrosion activity on the WE and if OCP < -254 mV vs. Ag/AgCl/KCl sat. there is 90% probability of having corrosion activity on the WE. Between these limits, there is uncertain corrosion activity.

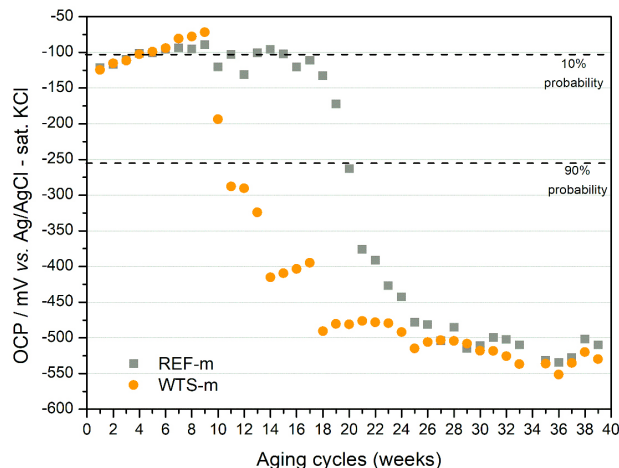


Figure 7. Evolution of the open circuit potential of working electrodes in REF and WTS-m versus $\text{Ag/AgCl/KCl}_{\text{sat}}$.

From Figure 7, one can see that the initial values for REF-m and WTS-m are similar and increased 100 mV from the first day to the sixth cycle together, suggesting the formation of a passivating layer, reducing corrosion risk. While WTS-m potential values increase a little more from the seventh to the ninth cycle, REF-m potential values started to stay constant, close to the threshold value for corrosion to become uncertain according to ASTM C876-15²⁴ from seventh to 17th cycle. This means that the passivation film on REF-m started to become unstable. WTS-m potential values decreased remarkably after the seventh cycle, indicating a corrosion activity after the 10th cycle. REF-m presented a similar decreasing behavior after the 18th cycle though and presented 90% probability of corrosion after the 20th cycle. Therefore, indicating that REF-m maintains the passivating film for a longer time on the steel, protecting it from corrosion for eight more weeks in the case of this test. The test was carried out for more 19 weeks after the samples presented 90% probability of corrosion and after 27 cycles, both REF-m and WTS-m corrosion potential values became similar, around -525 mV. This behavior was mentioned by other researchers.^{25,35,37,44} WTS-m showed to be more susceptible to corrosion activity, probably caused by the lower pH (Table 1) that WTS presents against the high alkalinity of the cement (approximately 12.5). Therefore, in this proportion of material to make WTS samples, it is not indicated to use this concrete in the marine environment. However, it is important to mention that is indicated to be used as reinforced concrete structure in urban areas by Brazilian standard NBR 6118.²⁸

After 39 weeks (cycles) of corrosion potential tests, mortars were opened to remove the steel bars to perform SEM analysis. Images were taken on steels from REF-m samples (REF) and steel from WTS-m (Figure 8). After

this time of immersion in chloride solution, the REF sample presents a structure formed on the surface clearly (Figure 8a), probably the oxides formed by corrosion, according to OCP measurements for this age. For the WTS sample (Figure 8b), the steel surface presented cracks beside the oxides. WTS-m samples started to corrode at least 5 weeks earlier than REF-m samples.

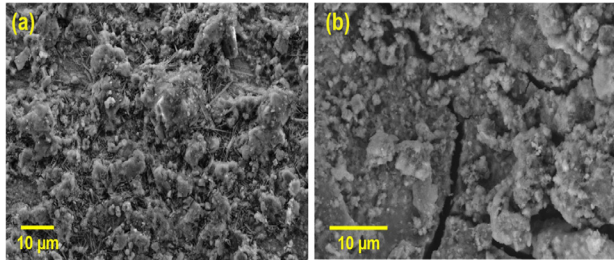


Figure 8. SEM images of (a) REF and (b) WTS steel samples after the end of the experiment.

Furthermore, knowing that the passivation film in WTS-m steel did not stabilize according to OCP monitoring in alkaline media, it is acceptable to conclude that this film broke easily, and the corrosion process occurred more quickly and intensely than in the REF sample.

Conclusions

In this paper, WTS was studied as a partial substitute of natural sand (3%), aiming the application of this waste at the civil construction. The compressive strength, modulus of elasticity and tensile strength showed a decrease of values when compared to the reference sample (REF). By EIS, the resistance of the cementitious matrix was not altered by WTS addition. Regarding steel resistance, the WTS may promote a higher susceptibility to frame corrosion, which can be correlated to the lower pH than REF medium. Due to these changes, WTS addition is not indicated for marine environment.

Although there is this limitation in the use of concrete with 3% WTS in place of sand, it can be used in urban areas. It is emphasized the fact that most cities in Brazil and in the world are not coastal, so there is a great potential for the application of this composite in civil construction. Especially, it should be noted that WTS is a waste that requires little processing before being used, therefore, it is cheaper than natural sand. In addition, it is possible to find WTS in all regions of Brazil, facilitating access and transport. For all the reasons mentioned, concrete with WTS incorporation is environmentally friendly and can be applied in civil construction.

Supplementary Information

Supplementary information, about São Carlos water treatment station (SAAE) plant, Mortar sample WTS and EIS measurements, is available free of charge at <https://jbcbsbq.org.br> as PDF file.

Acknowledgments

The authors thank the São Paulo Research Foundation (FAPESP) for the grant received (No. 2013/07296-2; No. 2018/16401-8), along with Coordenação de Aperfeiçoamento de Pessoal de Nível Superior (CAPES) (Finance Code 001) and MCTI/CNPq for their financial support (grants No. 303407/2020-4 and No. 307230/2018-0). Also, the authors thank the Laboratory of Structural Characterization (LCE/DEMa/UFSCar) for the general facilities.

Author Contributions

Mariana A. M. Rezende was responsible for investigation, methodology, data curation, writing- original draft preparation; Pedro P. Gromboni for investigation, methodology; Patricia G. Corradini for investigation, methodology, data curation, writing-original draft preparation, writing review and editing; Almir Sales for conceptualization, supervision, writing- reviewing and editing, project administration, resources; Lucia H. Mascaro for visualization, supervision, writing reviewing and editing.

References

1. Achon, C. L.; Barroso, M. M.; Cordeiro, J. S.; *Eng. Sanit. Ambient.* **2013**, *18*, 115. [Crossref]
2. Sales, A.; de Souza, F. R.; *Constr. Build. Mater.* **2009**, *23*, 2362. [Crossref]
3. Gomes, S. C.; Zhou, J. L.; Li, W.; Long, G.; *Resour., Conserv. Recycl.* **2019**, *145*, 148. [Crossref]
4. Eshtiaghi, N.; Markis, F.; Yap, S. D.; Baudez, J.-C.; Slatter, P.; *Water Res.* **2013**, *47*, 5493. [Crossref]
5. Sengupta, A. K.; Shi, B.; *J. AWWA* **1992**, *84*, 96. [Crossref]
6. Cucina, M.; Ricci, A.; Zadra, C.; Pezzolla, D.; Tacconi, C.; Sordi, S.; Gigliotti, G.; *Sci. Total Environ.* **2019**, *695*, 133762. [Crossref]
7. de Godoy, L. G. G.; Rohden, A. B.; Garcez, M. R.; da Costa, E. B.; Da Dalt, S.; Andrade, J. J. O.; *Constr. Build. Mater.* **2019**, *223*, 939. [Crossref]
8. González, K. B.; Pacheco, E.; Guzmán, A.; Avila Pereira, Y.; Cano Cuadro, H.; Valencia, J. A. F.; *Mater. Today Commun.* **2020**, *23*, 100930. [Crossref]

9. Torres, A.; Brandt, J.; Lear, K.; Liu, J.; *Science* **2017**, *357*, 970. [Crossref]
10. Beiser, V.; *Why the World is Running out of Sand*, <https://www.bbc.com/future/article/20191108-why-the-world-is-running-out-of-sand>, accessed in February 2023.
11. Niranjana, A.; *The World is Running Out of Sand*, <https://www.dw.com/en/sand-crisis-shortage-supply-mafia/a-56714226>, accessed in February 2023.
12. Statista, *Industrial Sand and Gravel Production Worldwide from 2010 to 2021*, <https://www.statista.com/statistics/728756/industrial-sand-and-gravel-production-worldwide/>, accessed in February 2023.
13. USGS; *Mineral Commodity Summaries*; National Minerals Information Center: Reston, 2022. [Link] accessed in February 2023
14. Kaish, A. B. M. A.; Odimegwu, T. C.; Zakaria, I.; Abood, M. M.; Nahar, L.; *Constr. Build. Mater.* **2021**, *284*, 122669. [Crossref]
15. Ching, C. Y.; Bashir, M. J. K.; Aun, N. C.; Aldahdooh, M. A. A.; *Constr. Build. Mater.* **2021**, *282*, 122703. [Crossref]
16. Cordeiro, J. S.; *Processamento de Lodos de Estações de Tratamento de Água (ETAs)*; RiMa: Rio de Janeiro, 2001.
17. ABNT NBR NM 67/1988: *Concreto - Determinação da Consistência pelo Abatimento do Tronco de Cone (Concrete - Slump Rest for Determination of the Consistency)*, Rio de Janeiro, 1998.
18. ABNT NBR 9479/2006: *Argamassa e Concreto - Câmaras Úmidas e Tanques para Cura de Corpos-de-Prova (Mortar and Concrete - Moist Rooms and Water Tanks for Curing)*, Rio de Janeiro, 2006.
19. ABNT NBR 5739/2018: *Concreto - Ensaio de Compressão de Corpos de Prova Cilíndricos (Concrete - Compression Test of Cylindrical Specimens)*, Rio de Janeiro, 2018.
20. ABNT NBR 8522/2017: *Concreto - Determinação dos Módulos Estáticos de Elasticidade e de Deformação à Compressão (Concrete - Determination of Static Modules of Elasticity and Compression Strain)*, Rio de Janeiro, 2017.
21. ABNT NBR 7222/2011: *Concreto e Argamassa - Determinação da Resistência À Tração por Compressão Diametral de Corpos de Prova Cilíndricos (Concrete and Mortar - Determination of the Tensile Strength by Diametrical Compression of Cylindrical Specimens)*, Rio de Janeiro, 2011.
22. ABNT NBR 9778/2005: *Argamassa e Concreto Endurecidos - Determinação da Absorção de Água, Índice de Vazios Massa Específica (Hardened Mortar and Concrete - Determination of Water Absorption, Voids and Specific Gravity)*, Rio de Janeiro, 2005.
23. ASTM G1-03: *Standard Practice for Preparing, Cleaning, and Evaluating Corrosion Test*, Philadelphia, 2017.
24. ASTM C876-15: *Standard Test Method for Corrosion Potentials of Uncoated Reinforcing Steel in Concrete*, Philadelphia, 2015.
25. Almeida, F. C. R.; Sales, A.; Moretti, J. P.; Mendes, P. C. D.; *Constr. Build. Mater.* **2015**, *82*, 31. [Crossref]
26. Moretti, J. P.; Sales, A.; Almeida, F. C. R.; Rezende, M. A. M.; Gromboni, P. P.; *Constr. Build. Mater.* **2016**, *113*, 317. [Crossref]
27. Liu, Y.; Zhuge, Y.; Chow, C. W. K.; Keegan, A.; Phan, P. N.; Li, D.; Quian, G.; Wang, L.; *Sci. Total Environ.* **2020**, 141182. [Crossref]
28. ABNT NBR 6118/2014: *Projeto de Estruturas de Concreto - Procedimento (Design of Concrete Structures - Procedure)*, Rio de Janeiro, 2014.
29. Huang, C.; Pan, J. R.; Sun, K.-D.; Liaw, C.-T.; *Water Sci. Technol.* **2001**, *44*, 273. [Crossref]
30. Wolff, E.; Schwabe, W. K.; Conceição, S. V.; *J. Cleaner Prod.* **2015**, *96*, 282. [Crossref]
31. Benlalla, A.; Elmoussaouiti, M.; Dahhou, M.; Assafi, M.; *Appl. Clay Sci.* **2015**, *118*, 171. [Crossref]
32. Liu, Y.; Zhuge, Y.; Chow, C. W. K.; Keegan, A.; Li, D.; Pham, P. N.; Huang, J.; Siddique, R.; *J. Environ. Manage.* **2020**, *262*, 110352. [Crossref]
33. El-Didamony, H.; Khalil, K. A.; Heikal, M.; *HBRC J.* **2014**, *10*, 73. [Crossref]
34. Hagemann, S. E.; Gastaldini, A. L. G.; Cocco, M.; Jahn, S. L.; Terra, L. M.; *J. Cleaner Prod.* **2019**, *214*, 916. [Crossref]
35. Ribeiro, D. V.; Labrincha, J. A.; Morelli, M. R.; *Cem. Concr. Res.* **2012**, *42*, 124. [Crossref]
36. Christensen, B. J.; Coverdale, T.; Olson, R. A.; Ford, S. J.; Garboczi, E. J.; Jennings, H. M.; Mason, T. O.; *J. Am. Ceram. Soc.* **1994**, *77*, 2789. [Crossref]
37. Ghorbani, S.; Taji, I.; Tavakkolizadeh, M.; Davodi, A.; de Brito, J.; *Constr. Build. Mater.* **2018**, *185*, 110. [Crossref]
38. Koga, G. Y.; Comperat, P.; Albert, B.; Roche, V.; Nogueira, R. P.; *Cem. Concr. Res.* **2019**, *122*, 212. [Crossref]
39. Poursaeed, A.; Hansson, C. M.; *Cem. Concr. Res.* **2009**, *39*, 391. [Crossref]
40. Kupwade-Patil, K.; Allouche, E. N.; *J. Mater. Civ. Eng.* **2013**, *25*, 1465. [Crossref]
41. Abu-Jdayil, B.; Mourad, A.-H.; Hussain, A.; *Constr. Build. Mater.* **2016**, *105*, 472. [Crossref]
42. Shi, J.; Ming, J.; Sun, W.; *Cem. Concr. Compos.* **2018**, *92*, 110. [Crossref]
43. Gromboni, M. F.; Sales, A.; Rezende, M. A. M.; Moretti, J. P.; Corradini, P. G.; Mascaro, L. H.; *J. Cleaner Prod.* **2021**, *284*, 124697. [Crossref]
44. Almeida, F. C. R.; Sales, A.; Moretti, J. P.; Mendes, P. C. D.; *Constr. Build. Mater.* **2019**, *226*, 72. [Crossref]

Submitted: November 5, 2022

Published online: February 23, 2023

